An Imbalance of IL-33/ST2-AXL-Efferocytosis Axis Induces Pregnancy Loss Through Metabolic Reprogramming of Decidual Macrophage

Yan-Ran Sheng
Obstetrics and Gynecology Hospital of Fudan University
Wen-Ting Hu
Obstetrics and Gynecology Hospital of Fudan University
Hui-Hui Shen
Obstetrics and Gynecology Hospital of Fudan University
Chun-Yan Wei
Obstetrics and Gynecology Hospital of Fudan University
Yu-Kai Liu
Obstetrics and Gynecology Hospital of Fudan University
Xiao-Qian Ma
Obstetrics and Gynecology Hospital of Fudan University
Ming-Qing Li
Obstetrics and Gynecology Hospital of Fudan University
Xiao-Yong Zhu (zhuxiaoyong@fudan.edu.cn)
Obstetrics and Gynecology Hospital of Fudan University https://orcid.org/0000-0002-2512-9703

Research Article

Keywords: Efferocytosis, IL-33/ST2 axis, Metabolic immune reprogramming, Decidual macrophages, Recurrent pregnancy loss

Posted Date: November 16th, 2021

DOI: https://doi.org/10.21203/rs.3.rs-1034014/v1

Version of Record: A version of this preprint was published at Cellular and Molecular Life Sciences on March 1st, 2022. See the published version at https://doi.org/10.1007/s00018-022-04197-2.

Abstract

During the implantation of embryo, apoptosis is inevitable. These apoptotic cells (AC) are removed by efferocytosis, which fills the macrophage with a metabolite load nearly equal to the phagocyte itself. A timely question pertains to the interrelationship between efferocytosis metabolism and the immune behavior of decidual macrophages (dMΦs) and its effect on pregnancy outcome. Here we report a positive feedback of IL-33/ST2-AXL-efferocytosis leading to pregnancy failure through metabolic reprogramming of dMΦs. We compared the serum level of IL-33, sST2, along with IL-33, ST2, efferocytosis and metabolism of dMΦs from both normal gravidas and unexplained recurrent pregnancy loss (RPL) patients. And we revealed the disturbance of IL-33/ST2 axis, increased apoptotic cells and elevated efferocytosis of dMΦs from the patients with RPL. Afterwards the dMΦs swallowing so many apoptotic cells secreted more sST2 and less TGF-β, which polarized dMΦs towards M1 phenotype. Moreover, the elevated sST2 biased the efferocytosis metabolism of RPL dMΦs towards oxidative phosphorylation and exacerbated the disruption of IL-33/ST2 signaling pathway. The metabolic disorders also led to the dysfunction of efferocytosis, resulting in more uncleared apoptotic cells and the secondary necrosis occurred. We also screened efferocytotic molecule AXL regulated by IL-33/ST2. This positive feedback of IL-33/ST2-AXL-efferocytosis led to pregnancy failure. And the IL-33 knockout mice demonstrated poor pregnancy outcomes, and exogenous supplementation of mouse IL-33 could partially alleviate the fate of embryo losses. These findings highlight a new etiological mechanism whereby dMΦs leverage immunometabolism for the homeostasis of microenvironment at the maternal-fetal interface.

Introduction

Efferocytosis is the clearance of dying and dead cells, which is performed by the professional and the nonprofessional phagocytes[1, 2]. This biological behavior has been artificially divided into recognition, engulfment and immunomodulation three steps involving several signals (“find-me”, “eat-me” and “don’t-eat-me” signals)[3]. There are a large number of cells undergoing apoptosis during embryonic development, and some studies have shown that a certain number of apoptotic cells (AC) at the maternal-fetal interface favor the invasion of trophoblast cells[4]. Decidual macrophages (dMΦs) and epithelial cells of the interface can clear these dying or dead cells to ensure success of pregnancy[5]. Deficiency or excessive efferocytosis should contribute to the origin and development of pathological pregnancies, such as unexplained recurrent pregnancy loss (RPL), preeclampsia, antiphospholipid syndrome, fetal growth restriction, rupture of ectopic pregnancy, and the research of its exact mechanisms is still at the early stage[6]. However, the efferocytosis metabolism and its roles in the maternal-fetal interface are still little known.

Interleukin-33 (IL-33) is an epithelial cell-derived cytokine that is released from the nucleus to the outside of cells in response to tissue injury, stress or infection, acting as an “alarmin” in the immune system. IL-33 exerts its biological function through binding to IL-1RL1 receptor (also known as ST2) and the coreceptor IL-1 receptor accessory protein (IL-1RAcP). Additionally, the secreted isoform of ST2 (also known as

sST2) is a decoy receptor for IL-33 and competing with membrane bound ST2 to block IL-33/ST2 signaling pathway[7]. It has been discovered that IL-33 is closely associated with trophoblast cell proliferation and placental growth[8]. Our previous work revealed that IL-33 derived from decidual stromal cells (DSCs) promoted the proliferation and invasion of DSCs via up-regulating chemokine CCL2/CCR2, and induced Th2 bias and suppressed cytotoxicity of decidual natural killer cells (dNKs)[9, 10]. And clinical study found that women with a viable fetus, but eventually miscarried, had dysregulated levels of serum IL-33, and potentially sST2 at six weeks' gestation[11]. Of note, IL-33/ST2 axis participates in regulating immune reprogramming of bone marrow-derived macrophages and FcεRIα$^+$ macrophages of squamous cell carcinoma through affecting macrophage metabolism[12, 13]. Therefore, it is attractive to speculate that similar activity may be existed between IL-33/ST2 signaling and the efferocytosis of dMΦs and the possible connections may play a significant role in maintaining the homeostasis at the maternal-fetal interface.

Herein, we focused on the effect of IL-33/ST2 axis on dMΦs efferocytosis and the underlying relationship between efferocytosis metabolism and the homeostasis of maternal-fetal interface. In current research, we elaborated a novel pathogenesis of pregnancy failure resulted from the disorder of IL-33/ST2 axis followed by a pathological positive feedback loop involving metabolism and polarization status of dMΦs at the maternal-fetal immune interface and clarified the molecule associated with efferocytosis downstream of IL-33/ST2 axis.

Materials And Methods

Tissue collection and primary isolation

Tissue samples used in this study were collected after obtaining the informed consent approved by Ethics Committee of Obstetrics and Gynecology Hospital, Fudan University. Decidual tissues were acquired from normal gestational women (normal group; n = 145; age, 28.0 ± 2.93 years, mean ± SD; gestational age, 52.34 ± 3.25 days) who chose elective vaginal termination for non-medical reasons from RPL patients (RPL group; n=72; age, 30.14 ± 3.07 years, mean ± SD; gestational age, 54.58 ± 3.57 days) who experienced the loss of two or more clinical pregnancies before 20 weeks of pregnancy, but not necessarily consecutive (documented by ultrasonography or histopathologic examination)[14]. Those patients who had abnormal vaginal bleeding, severe abdominal pain, or other typical symptoms of inflammation were excluded. Fresh decidual tissues were rinsed in 1×PBS twice to remove blood clots and finely minced within 60 min upon operation. Then, the decidual stromal cells (DSCs) and the decidual immune cells (DICs) were isolated and cultured as previously stated in detail[15].

Isolation, and treatment of decidual macrophages (dMΦs)

With the use of positive selection with anti-CD14 microbeads to isolate decidual macrophages from DICs according to the instruction of manufacturer (Cat#130-050-201, Miltenyi Biotec). The purity of enriched dMΦs reaches more than 90%, which were confirmed through flow cytometry[15]. The enriched dMΦs, as

well as cell line THP-1 were cultured in the complete RPMI 1640 medium with 10% FBS with or without the recombinant human ST2/IL-33R Fc Chimera (Cat#523-ST-100, R&D Systems), recombinant human IL-33 (Cat#3625-IL-010, R&D Systems), recombinant human GAS6 (Cat#885-GSB-050, R&D Systems), PI3K inhibitor LY294002 (Cat#S1737, Beyotime), AKT inhibitor Ⅷ (Cat#SF2784, Beyotime), MEK1/2 inhibitor U0126 (Cat#S1901, Beyotime), JNK inhibitor SP600125 (Cat#S1876, Beyotime), P38 MAPK inhibitor SB202190 (Cat#SC0380, Beyotime), and cultured at 37°C incubator under 5% CO2 for further processing.

Mice and IL-33 gene knockout (IL-33$^{-/-}$) C57BL/6J mice pregnant model

All experimental procedures that involved animals were performed in accordance with the Guide for the Care and Use of Laboratory Animals (China). The experimental methods in particular were carried out following the approved guidelines. IL-33$^{-/-}$ mice were established from Shanghai Model Organisms Center, Inc. 8-week-old wild type (WT) C57BL/6J ♀ mice and IL-33$^{-/-}$ ♂ mice were mated in a 2:1 ratio as control group. IL-33$^{-/-}$♀ mice and WT ♂ mice were mated 2:1 as the experimental group and sacrificed at 7.5 and 14.5 days after the appearance of vaginal plugs (G0.5 day). In parallel experiment, IL-33$^{-/-}$♀ mice were mated with WT ♂ mice and the IL-33$^{-/-}$♀ mice with vaginal plug were randomly divided into two groups randomly. One group of mice were injected intra-peritoneally with 100ul normal saline on the day of G3.5 day, 7.5day and 11.5day, set as control group. And the other group were intra-peritoneally injected with 200ng/100ul mouse IL-33 protein on the day of G3.5 day, 7.5day and 11.5day. Both group of mice were sacrificed at 14.5 days of gestation. And the pregnancy rate, embryo number, embryo absorption rate, crown-rump length and weight of embryos, diameter and weight of placentas of these groups was calculated. Moreover, minced uteri were digested in (DMEM)/F12 supplemented with 50% collagenase Type IV for 45 min at 37℃ with gentle agitation. The single-cell suspension of mice was filtered by 400 mesh sieve and for subsequent FCM assay.

Apoptotic assay

To obtain apoptotic DSCs, primary DSCs were incubated with cobalt chloride (CoCL2, 0-600uM, Cat#449776, Sigma) for 24 hours. After washing three times with PBS, digestion the cells with trypsin and evaluation with PE Annexin V Apoptosis Detection Kit (Cat#559763, BioLegend). The administration of CoCL2 resulted in increases in the number of apoptotic DSCs compared with those only treated with trypsin (60%-70% v.s.10%-20%). The apoptosis rate was defined as follows: (Annexin V $^{+}$7-AAD^{+} cells + Annexin V $^{+}$7-AAD^{-}cells)/total cells × 100%.

In vitro efferocytosis assay

In vitro efferocytosis assay, the apoptotic DSCs were labeled with CFSE Cell Division Tracker Kit (Cat# 423801, BioLegend) for 20 minutes at 37°C, following CFSE labeling, DSCs were incubated with dMΦs at a ratio of 2:1 (target: macrophage) for 120 minutes, at 37°C. The efficient efferocytosis rate was determined by flow cytometry, each data set was first gated on CD14-APC-positive macrophage. Efferocytosis rate was calculated as [CD14^{+}CFSE^{+} cells/CD14^{+} cells × 100%]. And in the assay with ST2-

OE THP-1, which could fluoresce spontaneously in green-FICT, the apoptotic DSCs were labeled with Tag-it Violet Proliferation and Cell Tracking Dye (Cat# 425101, BioLegend). Efferocytosis rate was determined as follows: $BV421^{+}FITC^{+}$ cells/$FITC^{+}$ cells × 100%.

Seahorse analysis

To measure the OCR and ECAR, normal dMΦs and RPL dMΦs were treated with apoptotic DSCs (AC) for 1 hour, and added to the XF96 cell culture microplates coated with CellTak (the number of dMΦs in each well was 1×10^5 and the number of AC was 5×10^4). OXPHOS was tested with the use of mitochondrial stress test kit (Cat#103015-100, Seahorse Bioscience), the following were injected: ATP-synthesis inhibitor oligomycin (1.5uM), carbonyl cyanide 4-(trifluoromethoxy) phenylhydrazone (FCCP; 1.5uM) to uncouple ATP synthesis, rotenone (100nM) to block complex I, and antimycin A (1uM) to block complex III. The glycolysis was measured using the glycolysis stress test kit (Cat#103020-100, Seahorse Bioscience), the following were injected successively in order: 20mM glucose, 1uM oligomycin (ATP synthesis inhibitor), and 80mM 2-DG (glycolysis inhibitor). The changes of OCR and ECRA were measure by Seahorse XF96 extracellular flux analyzer (Agilent Technologies). And the basic OCR, ATP production, max respiration of OXPHOS, spare capacity, basic ECAR, glycolysis, max respiration of glycolysis and glycolytic reserve were generated by Wave Desktop software (Agilent Technologies).

Mitochondrial Membrane Potential (mtΔΨ) Assay

The mitochondrial membrane potential (mtΔΨ) was detected with JC-1 (Cat#C2006, Beyotime). The dMΦs with or without AC were treated with 1×JC-1 dye for 20min followed by flow cytometry analysis. JC-1 is a fluorescent probe widely used to detect mitochondrial membrane potential. It has two forms of monomer and aggregates. Red fluorescence (Ex/Em=585/590nm) is the sign of active mitochondrial function and high mtΔΨ, while green fluorescence (Ex/Em=514/529nm) in the cells suggests poor mitochondrial function with low mtΔΨ. The red/green fluorescence ratio (590nm/529nm) indicated the value of mtΔΨ and the mitochondrial function.

Flow cytometry (FCM)

Cells were collected and incubated with corresponding fluorochrome-conjugated antibodies for 35 minutes at room temperature. As for the endonuclear IL-33 and intracytoplasmic TGF-β IFN-γ, we firstly fixed and permeabilized the cells with the use of BioLegend's FOXP3 Fix/Perm Buffer Set (Cat#421403). The fluorescent-labeled antibodies used in cells of human were as follows: CD14-APC-CY7 (Cat#301820), CD80-PE (Cat#305412), CD86-APC (Cat#305208), CD163-BV421 (Cat#333612), CD206-PE-CY7 (Cat#321124), all obtained from BioLegend; and ST2-PE (Cat#FAB5231P), IL-33-APC (Cat#IC3625A), AXL-PE (Cat#FAB154P) all purchased from R&D Systems. And the fluorescent-labeled antibodies applied in cells of mice were listed below: mCD45-BV421 (Cat#103126), mCD11/b-PE-CY7 (Cat#101216), mF4/80-FITC (Cat#123108), mTGF-β-PE (Cat#141305), mIFN-γ-BV421 (Cat#505842), mCD206-APC (Cat#141708), mCD86-BV421 (Cat#105032), mCD209-PE (Cat#833004), mCD80-APC (Cat#104713), all obtained from BioLegend; and mIL-33-PE (Cat#UC2744592, Introgen), mAXL-PE (Cat#FAB8541P, R&D Systems), PI3K-AF488 (CA#ab225371), p-PI3K-PE (CA#ab278691), AKT-AF488 (CA#5084S, CST), p-AKT-

PE (CA#558275, BD Pharmingen), ERK1/2-AF488 (CA#4780S, CST), p-ERK1/2-PE (CA#612566, BD Pharmingen). The samples were ran with the usage of CytoFlex analyzer (Beckman Coulter) and analyzed with FlowJo_V10 software for Windows (Tree Star, Inc.).

Enzyme linked immunosorbent assay (ELISA)

Cell supernatants were collected, centrifuged at 1000 g for 20 min to remove cell debris and collected the remaining supernatants for further assays. ELISA assay was performed to detect the titers of human IL-33 (Cat#42590, BioLegend), sST2 (Cat#DST200, R&D Systems), TGF-β (Cat#436707, BioLegend), and IFN-γ (Cat# 430104, BioLegend) according to the manufacturer's protocols.

Construction of stable ST2-overexpressing THP-1 cell line with lentivirus

THP-1 cells were obtained from Shanghai Institute for Life Science and maintained under standard culture conditions with RPMI 1640 medium (Cat#GNM-23471-S, Genom) and fetal bovine serum (FBS) (Cat#10099-141, Gibco) at 37°C with 95% normal air and 5% CO2. The lentiviral expression systems were purchased from Shanghai Genechem Co.,Ltd. The modeling multiplicities of infection (MOI) was 50. The viral infection enhancing reagent was HitransG A. After transfection, the virus media were harvested, and cells were treated for 72 hours with negative control (NC) lentivirus and ST over-expressed (ST2-OE) lentivirus, respectively. The negative control (NC) group and ST2-OE THP-1 treated with IL-33 (2ng/ml, 48h) were then detected for the RNA-Seq analysis (BerryGenonics company, NO: IBFC2018631).

RNA isolation and quantitative real-time PCR (qRT-PCR)

Total RNAs was extracted from cells with TRIzol (Cat#15596026, TAKARA) according to the manufacturer's protocol. The RNA was reversely transcribed to cDNA with the PrimeScriptTM RT reagent Kit (Cat#RR047A, TAKARA). And then semiquantitative qRT-PCR was performed with TB Green Premix Ex TaqII (Cat#RR820A, TAKARA). A comparative threshold cycle (CT) value was normalized to the values of GAPDH for each sample by using the $2^{-\triangle\triangle CT}$ method. The information of primers was listed in **Supplementary Table1**.

Western Blot

Radio-immunoprecipitation assay (RIPA) buffer (Cat#P0013B, Beyotime), along with protease inhibitor Cocktail (1:100, Cat#HY-K0010, MedChemExpress) and phosphatase inhibitor Cocktail □ (1:100, Cat#HY-K0022, MedChemExpress) were added into the cells and gained the total proteins. BCA Protein Assay Kit is used to measure protein concentration (Cat#P0010, Beyotime). GoldBand 3-color regular range protein marker (Cat#20351ES72, Yeasen) along with 10ug protein were separated through electrophoresis on the 10% polyacrylamide gels (Cat#P0012AC, Beyotime), then transblotted onto polyvinylidene difluoride membranes, followed by the incubation of antibodies against GAPDH (1:2000, Cat#5174, Cell Signaling Technology), ACTIN (1:2000, Cat#3700, Cell Signaling Technology), ST2 (1:1000, Cat# ab194113, Abcam), AXL (1:1000, Cat# ab227871, Abcam), p-AKT (1:2000, Cat#4060, Cell Signaling Technology), AKT (1:1000, Cat#4691, Cell Signaling Technology), Phospho-p44/42 MAPK (Erk1/2) (1:2000, Cat#4370,

Cell Signaling Technology), p44/42 MAPK (Erk1/2) (1:1000, Cat#4695, Cell Signaling Technology), p-JNK (1:1000, Cat#4668, Cell Signaling Technology), JNK (1:1000, Cat#9252, Cell Signaling Technology), p-P38 (1:1000, Cat#4511, Cell Signaling Technology), P38 (1:1000, Cat#8690, Cell Signaling Technology) at 4℃ overnight. Subsequently, the HRP-conjugated anti-rabbit IgG (1:3000, Cat#7074S, Cell Signaling Technology) or anti-mouse IgG (1:3000, Cat#7076S, Cell Signaling Technology) secondary antibodies were incubated with the membranes for one hour at the room temperature. Immunoreactive bands were visualized with the use of immobilon western HRP substrate luminol reagent (Cat#WBKlS0100, Millipore) in Amersham imaging system (General Electric). In the phosphorylation experiments, previous primary antibody and secondary antibody were stripped from PVDF membrane with the stripping buffer (Cat#WB6200, New Cell & Molecular Biotech) for 10 min. After re-blocked the membrane, another primary antibody was used to re-incubated with it at 4℃ overnight. Then the following steps were the same as described above.

The terminal deoxynucleotidyl transferase-mediated dUTP-biotin nick end labeling assay (TUNEL)

The 1 cm^3 of decidual tissues were obtained and fixed in 4% Paraformaldehyde Fix Solution (Cat# P0099, Beyotime), dehydrated in successive alcohol solutions, embedded in paraffin wax, and then sectioned for TUNEL staining. The TUNEL BrightGreen Apoptosis Detection Kit (Cat#A112, Vazyme) was used to detect the number of apoptotic cells of the decidual tissues according to the manufacturer's instructions.

Statistical analysis

The data were analyzed with GraphPad Prism 8 (GraphPad Software, La Jolla, CA), through unpaired Student's two-tailed t-test, one-way ANOVA or two-way ANOVA, according to test requirements. Each experiment was performed at least three separate occasions and the data were presented as the mean ± SD. *P < 0.05, ** P < 0.01, ***P < 0.001, **** P < 0.0001 were considered significant.

Results

The dMΦs from patients with unexplained RPL exhibit dysfunction of IL-33/ST2 axis and a mitochondrial bias during efferocytosis

To determine whether there would be potential clinical relevance of serum IL-33 or sST2 in RPL patients, we first measured IL-33 and soluble ST2 (sST2) levels in the serum of patients with unexplained RPL, using serum from normal pregnancy for comparison. We found that RPL patients show increased levels of sST2 when compared to normal pregnancy patients (Figure. 1B), while no difference in IL-33 levels was detected (Figure. 1A). As shown in Figure 1C, the expression level of IL-33 protein in dMΦs from unexplained RPL group was lower than that in the normal group. However, the ST2 expression of unexplained RPL group was increased (detected by flow cytometry, Figure 1D). Of note, the increased apoptotic cells in decidua and efferocytosis ability of dMΦs were observed in RSA patients (Figure 1E, F).

To explore the efferocytosis metabolism of dMΦs between normal pregnancy and RSA patients, we measured the oxygen consumption rate (OCR) and glycolytic extracellular acidification rate (ECAR) to reflect oxidative phosphorylation (OXPHOS) and glycolysis condition respectively. Compared with dMΦs from normal pregnancy, the basic OCR, ATP production, max respiration and mitochondrial spare capacity were significantly elevated in dMΦs from RSA patients during efferocytosis (Figure 1G). In contrast, the levels of basic ECAR, glycolysis, max respiration and the glycolytic reserve were obviously decreased in dMΦs from women with RPL (Figure 1H).

Dysfunction of IL-33/ST2 axis promoted DSCs apoptosis, dMΦs/THP-1 efferocytosis and led to an OXPHOS bias during efferocytosis

As previously mentioned, we observed that sST2 increases while IL-33 decreases in RPL dMΦs, and increased apoptotic cells in decidua tissue accompanies these alterations. To further examine how the dysregulation of the IL-33/ST2 balance contribute to RPL, we treated DSCs or dMΦs/THP-1 with sST2(200ng/ml,48h) for subsequent experiments.

As expected, exposure to sST2 led to the increased apoptosis of DSCs (Figure 2A). Additionally, treatment with sST2 promoted the efferocytosis of dMΦs from women with normal pregnancy (Figure 2B), suggesting that abnormal high level of sST2 should contribute to the high apoptosis and efferocytosis in decidua from unexplained RPL patients by interfering the IL-33/ST2 signaling.

Mitochondrial membrane potential (mtΔΨ) was obviously decreased in dMΦs from women with unexplained RPL (Figure 2C). And THP-1 displayed the same results (Figure 2D, E). More importantly, IL-33 promoted a glycolytic bias while sST2 induced a mitochondrial bias during efferocytosis of dMΦs (Figure 2F, G) and THP-1 cells (Figure 2H, I). These findings suggest that dysfunction of IL-33/ST2 axis occurred in the RPL patients, induces more apoptotic cells and higher efferocytosis ability with an OXPHOS bias.

Efferocytosis is more dependent on glycolysis than OXPHOS

Owing to the disruption of energy metabolism of dMΦs from patient with unexplained RPL, we further investigate the possible metabolic mechanism on the efferocytosis of macrophages. 2-Deoxy-D-glucose (2-DG) is a glucose analog that acts as a competitive inhibitor of glucose metabolism. Further analysis showed that the glycolytic level of THP-1 cells decreased immediately after 2-DG treatment, while 2-DG did not inhibit glycolytic metabolism after 24h and 48h treatment (Figure 3A). In the subsequent experiments, therefore, 2-DG was added at the beginning of the efferocytosis assay, and it inhibited the efferocytosis of THP-1 cell line as well as dMΦs (Figure 3B, C). However, OXPHOS inhibitor oligomycin had no such effect (Figure 3D, E).

IL-33 deficiency increases the risk of pregnancy failure

Subsequently, the terminal deoxynucleotidyl transferase-mediated nick end labeling (TUNEL) assay was carried out in WT and IL-33$^{-/-}$ pregnant mice model to measure the apoptotic cells at the maternal-fetal interface. To eliminate the interference of embryo genotypes, we observed the apoptotic cells in WT ♀ mice and IL-33$^{-/-}$ ♂ mice mating model and IL-33$^{-/-}$♀ mice and WT ♂ mice mating model, and found there was no significant difference in the number of apoptotic cells between WT and IL-33$^{-/-}$ pregnant mice at G7.5 days (Figure 4A). However, the number of apoptotic cells was markedly increased in IL-33$^{-/-}$ pregnant mice at G14.5 day (Figure 4B), suggesting that macrophages in mouse uterus (uMΦs) should compensate for the removal of increased apoptotic cells during early pregnancy, and the elevated efferocytosis might be a secondary reaction to the high apoptosis. Meanwhile, the uMΦs from IL-33$^{-/-}$ pregnant mice had a pro-inflammatory M1 bias phenotype (CD80^{high}CD86^{high}IFN-γ^{high}CD206^{low}CD209^{low}TGF-β^{low}), especially at G7.5 days (Figure 4C, D **and Figure. S1)**.

Notably, we observed that the pregnant rate of IL-33$^{-/-}$ mice was relatively low (Figure 4E). Compared with the WT pregnant mice, additionally, the IL-33$^{-/-}$ pregnant mice had a lower implantation number (Figure 4F) and high embryo absorption rate, lower crown-rump length and weight of embryos, lower diameter and weight of placentas (Figure 4G). These data indicate that IL-33 deficiency led to excessive apoptotic cells and elevated efferocytosis at the mater-fetal interface, and poor pregnancy outcomes.

DMΦs from unexplained RPL patients is prone to the persistent M1 imbalance and high sST2 after efferocytosis

Efferocytosis fills the macrophage with a metabolite load nearly equal to the phagocyte itself. Moreover, the impact of efferocytosis metabolism on the immunological function of macrophages has been revealed resent years[16, 17].To explore the potential effect of efferocytosis on polarization of dMΦs, we analyzed the expression of the M1/M2-related molecules of dMΦs before and after efferocytosis. Before the efferocytosis, dMΦs from women with normal pregnancy displayed a M2 bias phenotypes, but there was a M1 phenotype in dMΦs from women with RPL. These results echoed our previous results[15]. After efferocytosis, the expression of these molecules decreased significantly both in normal and RPL dMΦs. More importantly, the superiority of M1 bias continued to expand (CD80^{high}CD86^{high}CD206^{low}CD209^{low}) after efferocytosis of dMΦs from women with RPL (Figure 5A). Additionally, other pro-inflammatory markers such as iNOS, IL1-β and TNF-α were tested by RT-PCR (Figure 5B). Similarly, these classical pro-inflammatory molecules (iNOS and TNF-α) did not decrease significantly in RPL dMΦs after efferocytosis.

Further, we detected the secretion of IL-33, sST2, TGF-β and IFN-γ of dMΦs before and after efferocytosis. IL-33 secreted by dMΦs was relatively low, which also was consistent with our previous report. DSCs were one of the main sources of IL-33 at the maternal-fetal interface[10]. After efferocytosis, IL-33 secretion was increased, but there was no statistical significance (Figure 5C). After efferocytosis, RPL dMΦs secreted higher level of sST2 (Figure 5D), and thereby exerted the blocking effect of IL-33/ST2 signal transduction. Normal dMΦs secreted higher level of TGF-β before and after efferocytosis, which should be helpful to

the invasion of trophoblasts and embryonic growth and development (Figure 5E)[18]. In addition, RPL dMΦs secreted higher level of IFN-γ before and after efferocytosis (Figure 5F)[19], although its concentration was too infinitesimal. The results suggest that dMΦs from RPL patients have a persistent M1 bias and high sST2 after efferocytosis.

IL-33 suppresses efferocytosis of dMΦs by down-regulating the expression of efferocytosis-related receptor AXL

To further investigate the regulatory mechanism of IL-33/ST2 on efferocytosis of dMΦs, ST2-overexpressed (ST2-OE) THP-1 cells were constructed **(Figure S2A, B)**. The negative control (NC) group and ST2-OE THP-1 treated with IL-33 were then detected for the RNA-Seq analysis. Compared with the NC group, there were 1131 genes with high expression and 16 genes with low expression in the ST2-OE group **(Figure S2C)**. Based on the differential expression genes, three signal pathways (i.e., inflammatory pathway, phagocytosis pathway, and the endocytosis pathway) were enriched by the Gene Ontology (GO) annotation (Figure 6A). Among these genes, the complement C3 and the efferocytosis-related receptor AXL should be emphasized, which were involved in the three signaling pathways (Figure 6B). Subsequently, the results of qRT-PCR confirmed that ST2-OE group of THP-1 cells had low levels of C3 and AXL **(Figure S2D)**. The Tyro3, AXL and MerTK (TAM) tyrosine kinases, are a family of efferocytosis receptors. They can recognize apoptotic cells indirectly through binding to the phosphatidylserine (PtdSer) with the two binding serum proteins growth arrest-specific protein 6 (GAS6) and the vitamin K-dependent factors protein S (PROS1)[20, 21]. In addition, AXL and MerTK are particularly important for efferocytosis in dendritic cells and macrophages[22]. Interestingly, ST2-OE group did not influence the expression of other efferocytosis-related receptors, such as Tyro3, MerTK, and CD300A **(Figure S2D)**.

Subsequently, we observed that $CD14^+$ dMΦs from patients with unexplained RPL had higher level of AXL (Figure 6C), which was consistent with the high efferocytosis ability of dMΦs from RPL patients. More importantly, treatment with IL-33 up-regulated the expression of AXL and the efferocytosis ability of dMΦs and THP-1 and sST2 had the opposite effect (Figure 6D, E **and Figure S2E, F)**. However, the efferocytosis of dMΦs and THP-1 cells did not response to exogenously GAS6 (Figure 6F **and Figure S2G)**. These data indicate that AXL should be involved in the regulation effect of IL-33/ST2 axis on efferocytosis of dMΦs.

The IL-33/ST2 axis inhibits AXL expression of dMΦs via activating PI3K/AKT and ERK1/2 signaling pathways

To explore the signal transduction mechanism of the IL-33/ST2 axis and AXL, the pathway enrichment of differential expression genes of the RNA-seq data was analyzed. As shown, the PI3K/AKT and MAPK signaling pathways were mainly activated after IL-33 treatment of ST2-OE THP-1 cells (Figure 7A). Further analysis showed that stimulation of IL-33 up-regulated AXL expression and the phosphorylation levels of AKT and ERK1/2, but not JNK and P38 **(Figure S3A, B)**. Additionally, blocking the PI3K/AKT or ERK1/2 signaling pathway could reverse the stimulatory effect of IL-33 on AXL expression in dMΦs and

THP-1 cells (Figure 7D-F, **and Figure S3C)**. However, treatment with the P38 inhibitor or JNK inhibitor had not similar effect (Figure 7B-C). We also observed that blocking the PI3K/AKT or ERK1/2 signaling pathway enhanced the efferocytosis of dMΦs and THP-1 cells (Figure 7G **and Figure S3D)**. Clinically, we tested the percentages of p-PI3K, p-AKT and p-ERK in the dMΦs from normal and RPL patients. We found that RPL dMΦs showed lower phosphorylation of PI3K, AKT and ERK compared with normal dMΦs (Figure 7H). In animal study, we also discovered the lower phosphorylation of AKT and ERK in the IL-33$^{-/-}$ mice **(Figure S3E, F)**. And the treatment of sST2 on normal dMΦs reduced the phosphorylation levels of PI3K, AKT and ERK, while the effect of IL-33 was inconsistent with our expectations (Figure 7H). And there were no significant differences of PI3K inhibitor or AKT inhibitor or ERK inhibitor on the OXPHOS and glycolysis in normal dMΦs **(Figure S3G, H)**. We considered that there might be other pathways involved. Further protein-protein interaction network prediction analysis by the STRING database (https://www.string-db.org/) was performed **(Figure S3I)**. And Aryl Hydrocarbon Receptor (AHR), which plays an important regulatory role in a variety of biological functions of macrophage[23–25], may also be involved in the regulation of IL-33 on AXL and efferocytosis metabolism in macrophage. And this remains to be further studied. These data suggest that the suppression of IL-33 on efferocytosis of dMΦs is dependent on the down-regulation of AXL mediated by the PI3K/AKT and ERK1/2 signaling pathways.

Exogenous IL-33 prevents pregnant failure of IL-33$^{-/-}$ pregnant mice

To further confirm the roles of IL-33 on the efferocytosis of dMΦs and normal pregnancy, the IL-33$^{-/-}$♀ mice were mated with WT♂ mice, and then injected intra-peritoneally with or without recombinant mouse IL-33 protein (IL-33 group). As expected, supplementation with exogenous IL-33 significantly decreased the number of apoptotic cells at the maternal-fetal interface of IL-33$^{-/-}$ pregnant mice (Figure 8A). The CD45^{+}F4/80^{+}CD11/b^{+} uMΦs of IL-33 group expressed lower AXL (Figure 8B**).** In addition, these uMΦs displayed M2 phenotype (CD80^{low}CD86^{low}IFn-γ^{low}CD209^{high}TGF-β^{high}) in IL-33 group (Figure 8C **and Figure S1C).** More importantly, the embryo absorption rate, crown-rump length and weight of embryos, diameter and weight of placentas were improved in IL-33$^{-/-}$ pregnant mice with peritoneal injection of IL-33, although there was no statistical difference in the number of embryo implantation (Figure 8D). These results demonstrate that exogenous IL-33 supplementation improves pregnancy outcomes of IL-33$^{-/-}$ pregnant mice, and this effect should be dependent on inhibiting apoptosis and the expression of AXL and triggering the M2 bias of uMΦs.

Discussion

Apoptosis in early embryogenesis is inevitable and necessary. Too many or too few apoptotic cells lead to pregnancy failure[4, 26]. Efferocytosis has a central role in scavenging apoptotic cells in differentiated tissues[5, 27]. Decidual macrophages, as the most antigen presenting cells at the maternal-fetal interface, are the main operators of efferocytosis. However, how efferocytosis and the following metabolic and immunological changes of dMΦs function in this particular microenvironment remains unknown. Here,

we found that the immunological phenotypes of dMΦs from normal and unexplained RPL patients were different after efferocytosis. The RPL dMΦs with M1 phenotype did not convert to M2 phenotype after efferocytosis. It has been reported that efferocytosis of necrotic debris promotes the occurrence of inflammatory response[28, 29]. These findings led us to speculate that there might be different reactions of efferocytosis, the death mode of the engulfed cells or the functional status of phagocytes themselves may determine the function of efferocytosis, and the ultimate purpose of efferocytosis is to maintain the homeostasis of the local microenvironment.

The dMΦs at the maternal-fetal interface account for 20% of the total number of decidual immune cells, which have a strong plasticity and heterogeneity, and play an important role in maintaining immune tolerance, protecting fetus from infection, removing the apoptotic cell[30, 31] and remodeling of the helical arterioles[32]. Therefore, rather than functioning as antigen presenting cells, dMΦs should be considered as cellular transducers more broadly that perceive sensory stimuli (such as invading trophoblast cells and apoptotic DSCs) and make responses to maintain the homeostasis of the maternal-fetal interface.

The adaptation of each type of macrophages to the metabolic environment is closely related to their main functions, and the metabolism of M1 and M2 macrophages is also different[33]. It was initially believed that pro-inflammatory M1 type macrophages mainly rely on aerobic glycolysis for energy supply, and this metabolic characteristic is conducive to a rapid production of ATP by macrophages to maintain their phagocytosis and scavenging function[34]. In these macrophages, HIF-1α is activated and plays a key role in the process of glycolysis[35]. On the contrary, anti-inflammatory M2 macrophages have a complete TCA cycle, fatty acid oxidation (FAO) and OXPHOS[33]. However, some recent studies revealed that the differentiation of M2-type macrophages also requires glycolysis to support for fatty acid synthesis and OXPHOS of M2, and it was found that FAO also exists in M1 macrophages to facilitate the activation of their inflammasomes[36]. IL-33/ST2 axis has also been found to regulate the differentiation of macrophages through metabolism. The disorder of IL-33/ST2 axis enhances the OXPHOS level of macrophages, and decrease the glucose uptake and ECAR value. The number of mitochondria and DNA copy are increased, and the expression of mitochondrial fusion-related genes are increased[13]. Inconsistently, IL-33/ST2 axis is also reported to promote glycolysis, inhibit OXPHOS and promote M2 polarization of macrophages through mTOR pathway, promoting the occurrence and development of tumors[7]. These findings above suggest a more complex metabolic network during macrophage activation, and macrophages of different tissues and organs have metabolic heterogeneity. In current research, the activation of IL-33/ST2 was able to polarize dMΦs towards M2 bias and restrict glycolysis-mediated efferocytosis. After efferocytosis, the phenotype of dMΦs remain tolerant, contributing to maintenance of normal pregnancy. Moreover, the elevated sST2 biased the efferocytosis metabolism of RSA dMΦs towards OXPHOS and exacerbated the disruption of IL-33/ST2 signaling pathway. The metabolic disorders, in turn, led to the dysfunction of efferocytosis, resulting in more uncleared apoptotic cells and excessive secondary necrosis. Our previous reported showed IL-33 also promoted the proliferation and invasion of DSCs[9]. As expected, we observed that knock out of IL-33 increased the risk of pregnant loss with higher apoptotic cells and M1 polarization of dMΦs.

As the other molecule found in RNA-seq analysis along with AXL, the role of complement C3 in pregnancy has been investigated in many studies. In the early stage of human embryo development, each component of the complement system has begun to be synthesized. The complement at maternal-fetal interface has an important influence on the formation of placenta[37], and the disorder of the complement system can also promote the occurrence and development of eclampsia[38]. Meanwhile, the activation of complement system is vital for maintaining host defense and fetal survival. Some studies have shown that the occurrence of spontaneous abortion is related to low complement level[39]. In the rat model of pregnancy, it was found that the content of complement C3 in yolk sac after embryo implantation was rich, which played an important role in promoting the growth and development of embryos[40].In the pregnant mouse models, placental growth restriction may lead to the development of eclampsia due to deficiency of complement C3 and C1q[38]. In addition, a cohort study with full exon Sanger sequencing of all C3 encoding genes in patients with recurrent abortion identified several heterozygous nonsynonymous mutations of C3 encoding genes. The recombinant expression of these mutations can affect the secretion and function of complement C3 protein, and may be one of the etiologies of RPL[41]. A recent clinical study focusing on the markers of neural tube defects (NTDs) in the process of embryonic development have found that in the process of normal pregnancy, some complement components (such as C3 and C9, C1R) content in maternal circulation system increased, guessing that the abnormal expression of complement protein C3 and C9 might be involved in the development of NTDs in the process of embryonic development. These proteins may be used as biomarkers for early non-invasive diagnosis of NTDs[42]. A recent study found that iC3b, one of the hydrolysates of complement C3, was very important for the maintenance of normal pregnancy. The mechanism is that complement receptors (such as CR3) on the surface of decidual macrophages can recognize iC3b and promote the clearance of apoptotic cells[43].

AXL mediates the “eat-me” signal during efferocytosis. It inhibits the development of inflammation and mediates tissue repair through efferocytosis and mediates immunosuppression in the tumor microenvironment, which is associated with poor prognosis of tumors[20]. Clinical studies found that in plasma of severe preeclampsia patients, free MerTK and AXL expression increases, and positively correlated with the severity of blood pressure and proteinuria. The GAS6 was lower, and negatively correlated to the level of proteinuria, suggesting TAM related signaling pathways (especially AXL-GAS6 signaling pathway) might participate in the pathological process of preeclampsia[44]. In addition, clinical cohort studies found that AXL-mediated Zika virus infection leads to the occurrence of congenital microcephaly[45]. Although it has been reported that Zika virus infection in mouse model did not require the TAM receptor family to mediate[46], and knockout of AXL did not prevent Zika virus infection of human neural progenitor cells and brain[47]. As the other molecule obtained by Venn diagram with complement C3, we speculate that AXL might also affect the microenvironment at the maternal-fetal interface. Therefore, AXL was selected as the follow-up molecule downstream of IL-33/ST2. Herein, we revealed the regulation of IL-33/ST2 on AXL and the affection on the pregnancy outcome for the first time.

Notably, we found IL-33 down-regulated the expression of AXL but not MerTK, and GAS6 was not involved in the regulation of efferocytosis in dMΦs. The downstream signaling pathways of IL-33/ST2 include ERK1/2, JNK, P38/MAPK, PI3K/AKT, and NF-κB[48], which are involved in the regulation of pro-inflammatory and anti-inflammatory responses in various microenvironments. In this study, we found that IL-33/ST2 decreased the expression of AXL in dMΦs by activating PI3K/AKT and ERK1/2 signaling pathway. And these two signaling pathways have also been widely reported in the etiology of RPL[49–51], suggesting that inactivation of PI3K/AKT and ERK1/2 signaling pathway should contribute to spontaneous abortion by an imbalance of efferocytosis. *In vivo* confirmation trials, we observed that administration with IL-33 led to the decrease of AXL, the increase of M2 differentiation, homeostasis of efferocytosis at the maternal-fetal interface, and improved the pregnant outcome of IL-33$^{-/-}$ mice.IL-33 can be found in various cells including mastocyte, dendritic cell and adipocyte. It acts an active part in inducing immunotolerance and immunoregulation, which can be used for preparing the medicine for treating the autoimmune disease. Similarly, we have found blocking IL-33/ST2 axis is promising to improve the outcome of miscarriage. Our hypothesis is based on clinical observations related to the IL-33/ST2 axis with some diseases, and we extend these discoveries to the clinical patients with unexplained RPL. More importantly, sST2 has been considered as an important prognostic marker and indicators for monitoring therapy in patients with heart failure, and its relatively mature clinical detection methods[52]. Interestingly, sST2 is expected to be a promising predictor of clinical abnormal pregnancy, such as pre-eclampsia and miscarriage. The circulating and placenta sST2 were increased in pre-eclampsia, although plasma IL-33 level showed no significant difference[53]. Additionally, the predictive value of IL-33/ST2 was reported for miscarriage at 6 weeks of gestation[11]. As expected, we observed that increased ST2 levels in patients with missed abortion in this study. Notably, efferocytosis-targeted strategies are emerging on tumorigenesis and cancer management[3, 54]. In current study, the “eat-me” signaling AXL is considered as a downstream regulatory molecule of IL-33/ST2 in dMΦs. Therefore, the potential value of targeting IL-33/sST2 axis and AXL in warning and intervention of unexplained RPL should be emphasized. However, due to the limited number of clinical samples in this study, the potential value of sST2 in waring of unexplained RPL needs to be validated with a large sample of clinical data in the future.

Conclusions

In conclusion, we described a complex regulatory network interacting between efferocytosis and metabolism of dMΦs at the maternal-fetal microenvironment **(Figure S4)**. Under normal condition, the IL-33/ST2 axis activates the ERK/2 and PI3K/AKT signal pathways to down-regulate the expression of AXL, thereby restricting the redundant efferocytosis to ensure a certain number of apoptotic cells at the maternal-fetal interface. Additionally, the activation of IL-33/ST2 was able to polarize dMΦs towards a M2 bias and control the efferocytosis dominated by glycolysis, which is beneficial to the maternal-fetal immunotolerance of normal pregnancy. Once the IL-33/ST2 axis is disturbed, the number of apoptotic cells increased, and the efferocytosis function of dMΦs was secondarily enhanced. The dMΦs with higher efferocytosis will secrete more sST2 and less TGF-β, which polarized dMΦs towards a M1 phenotype.

The elevated sST2 further disrupted efferocytosis of dMΦs towards OXPHOS and exacerbated the disruption of IL-33/ST2 signaling pathway. The metabolic disorders also led to the dysfunction of efferocytosis, resulting in more uncleared apoptotic cells and secondary necrosis, and eventually leading to the occurrence of spontaneous abortion. This study provides a novel mechanism of the immune etiology of recurrent spontaneous abortion from the perspective of efferocytosis metabolism.

Declarations

* Ethics approval and consent to participate

Tissue samples used in this study were collected after obtaining the informed consent approved by Ethics Committee of Obstetrics and Gynecology Hospital, Fudan University.

* Consent for publication

All authors agree to publish in the journal of ***Cellular and Molecular Life Sciences.***

* Availability of data and material

Not applicable.

* Competing interests

The authors declare no conflict of interest.

* Funding

This research was funded by the National Natural Science Foundation of China (NSFC 81871143, 82071624, 31800768, 92057119, and 31970798), the Program for Zhuoxue of Fudan University (JIF157602) andthe Support Project for Original Personalized Research of Fudan University.

* Authors' contributions

Yan-Ran Sheng performed experiments, data analysis, generated figures and prepared manuscript; Wen-Ting Hu designed the study performed experiments and assisted with data interpretation; Hui-Hui Shen performed experiments, searched the literatures and edited the manuscript; Chun-Yan Wei, Yu-Kai Liu, Xiao-Qian Ma searched the literatures; Ming-Qing Li designed the study, guided experiments and edited the manuscript; Xiao-Yong Zhu initiated and supervised the study and edited the manuscript.

* Acknowledgements

All authors thank all the participants involved in this study, especially Miss. Taniya from Albania for editing English Language and spelling.

References

[1] DORAN A C, YURDAGUL A, JR., TABAS I. Efferocytosis in health and disease [J]. Nature reviews Immunology, 2020, 20(4): 254-67.https://doi.org/10.1038/s41577-019-0240-6

[2] BOADA-ROMERO E, MARTINEZ J, HECKMANN B L, et al. The clearance of dead cells by efferocytosis [J]. Nature reviews Molecular cell biology, 2020, 21(7): 398-414.https://doi.org/10.1038/s41580-020-0232-1

[3] ZHOU Y, YAO Y, DENG Y, et al. Regulation of efferocytosis as a novel cancer therapy [J]. Cell communication and signaling : CCS, 2020, 18(1): 71.https://doi.org/10.1186/s12964-020-00542-9

[4] VON RANGO U, KRUSCHE C A, KERTSCHANSKA S, et al. Apoptosis of extravillous trophoblast cells limits the trophoblast invasion in uterine but not in tubal pregnancy during first trimester [J]. Placenta, 2003, 24(10): 929-40.https://doi.org/10.1016/s0143-4004(03)00168-1

[5] HOIJMAN E, HäKKINEN H-M, TOLOSA-RAMON Q, et al. Cooperative epithelial phagocytosis enables error correction in the early embryo [J]. Nature, 2021, 590(7847): 618-23.https://doi.org/10.1038/s41586-021-03200-3

[6] SHENG Y R, HU W T, WEI C Y, et al. Insights of efferocytosis in normal and pathological pregnancy [J]. American journal of reproductive immunology (New York, NY : 1989), 2019, 82(2): e13088.https://doi.org/10.1111/aji.13088

[7] XU H, LI D, MA J, et al. The IL-33/ST2 axis affects tumor growth by regulating mitophagy in macrophages and reprogramming their polarization [J]. Cancer biology & medicine, 2021, 18(1): 172-83.https://doi.org/10.20892/j.issn.2095-3941.2020.0211

[8] FOCK V, MAIRHOFER M, OTTI G R, et al. Macrophage-derived IL-33 is a critical factor for placental growth [J]. Journal of immunology (Baltimore, Md : 1950), 2013, 191(7): 3734-43.https://doi.org/10.4049/jimmunol.1300490

[9] HU W T, LI M Q, LIU W, et al. IL-33 enhances proliferation and invasiveness of decidual stromal cells by up-regulation of CCL2/CCR2 via NF-κB and ERK1/2 signaling [J]. Molecular human reproduction, 2014, 20(4): 358-72.https://doi.org/10.1093/molehr/gat094

[10] HU W T, HUANG L L, LI M Q, et al. Decidual stromal cell-derived IL-33 contributes to Th2 bias and inhibits decidual NK cell cytotoxicity through NF-κB signaling in human early pregnancy [J]. Journal of reproductive immunology, 2015, 109(52-65.https://doi.org/10.1016/j.jri.2015.01.004

[11] KAITU'U-LINO T J, TUOHEY L, TONG S. Maternal serum interleukin-33 and soluble ST2 across early pregnancy, and their association with miscarriage [J]. Journal of reproductive immunology, 2012, 95(1-2): 46-9.https://doi.org/10.1016/j.jri.2012.06.003

[12] TANIGUCHI S, ELHANCE A, VAN DUZER A, et al. Tumor-initiating cells establish an IL-33-TGF-β niche signaling loop to promote cancer progression [J]. Science (New York, NY), 2020, 369(6501): 10.1126/science.aay1813

[13] XU H, SUN L, HE Y, et al. Deficiency in IL-33/ST2 Axis Reshapes Mitochondrial Metabolism in Lipopolysaccharide-Stimulated Macrophages [J]. Frontiers in immunology, 2019, 10(127.https://doi.org/10.3389/fimmu.2019.00127

[14] VAN DIJK M M, KOLTE A M, LIMPENS J, et al. Recurrent pregnancy loss: diagnostic workup after two or three pregnancy losses? A systematic review of the literature and meta-analysis [J]. Human reproduction update, 2020, 26(3): 356-67.https://doi.org/10.1093/humupd/dmz048

[15] SHENG Y R, HU W T, WEI C Y, et al. IL-33/ST2 axis affects the polarization and efferocytosis of decidual macrophages in early pregnancy [J]. American journal of reproductive immunology (New York, NY : 1989), 2018, 79(6): e12836.https://doi.org/10.1111/aji.12836

[16] ZHANG S, WEINBERG S, DEBERGE M, et al. Efferocytosis Fuels Requirements of Fatty Acid Oxidation and the Electron Transport Chain to Polarize Macrophages for Tissue Repair [J]. Cell metabolism, 2019, 29(2): 443-56.e5.https://doi.org/10.1016/j.cmet.2018.12.004

[17] MORIOKA S, PERRY J S A, RAYMOND M H, et al. Efferocytosis induces a novel SLC program to promote glucose uptake and lactate release [J]. Nature, 2018, 563(7733): 714-8.https://doi.org/10.1038/s41586-018-0735-5

[18] LI Y, YAN J, CHANG H M, et al. Roles of TGF-β Superfamily Proteins in Extravillous Trophoblast Invasion [J]. Trends in endocrinology and metabolism: TEM, 2021, 32(3): 170-89.https://doi.org/10.1016/j.tem.2020.12.005

[19] QIN S, ZHANG Y, ZHANG J, et al. SPRY4 regulates trophoblast proliferation and apoptosis via regulating IFN-γ-induced STAT1 expression and activation in recurrent miscarriage [J]. American journal of reproductive immunology (New York, NY : 1989), 2020, 83(6): e13234.https://doi.org/10.1111/aji.13234

[20] DAVRA V, KUMAR S, GENG K, et al. Axl and Mertk receptors cooperate to promote breast cancer progression by combined oncogenic signaling and evasion of host anti-tumor immunity [J]. Cancer research, 2020, 10.1158/0008-5472.Can-20-2066

[21] TANAKA M, SIEMANN D W. Gas6/Axl Signaling Pathway in the Tumor Immune Microenvironment [J]. Cancers, 2020, 12(7): 10.3390/cancers12071850

[22] MYERS K V, AMEND S R, PIENTA K J. Targeting Tyro3, Axl and MerTK (TAM receptors): implications for macrophages in the tumor microenvironment [J]. Molecular cancer, 2019, 18(1): 94.https://doi.org/10.1186/s12943-019-1022-2

[23] YANG X, LIU H, YE T, et al. AhR activation attenuates calcium oxalate nephrocalcinosis by diminishing M1 macrophage polarization and promoting M2 macrophage polarization [J]. Theranostics, 2020, 10(26): 12011-25.https://doi.org/10.7150/thno.51144

[24] SHINDE R, HEZAVEH K, HALABY M J, et al. Apoptotic cell-induced AhR activity is required for immunological tolerance and suppression of systemic lupus erythematosus in mice and humans [J]. Nature immunology, 2018, 19(6): 571-82.https://doi.org/10.1038/s41590-018-0107-1

[25] CAMPESATO L F, BUDHU S, TCHAICHA J, et al. Blockade of the AHR restricts a Treg-macrophage suppressive axis induced by L-Kynurenine [J]. Nature communications, 2020, 11(1): 4011.https://doi.org/10.1038/s41467-020-17750-z

[26] PAPARINI D, GRASSO E, CALO G, et al. Trophoblast cells primed with vasoactive intestinal peptide enhance monocyte migration and apoptotic cell clearance through αvβ3 integrin portal formation in a model of maternal-placental interaction [J]. Molecular human reproduction, 2015, 21(12): 930-41.https://doi.org/10.1093/molehr/gav059

[27] AKHTAR N, LI W, MIRONOV A, et al. Rac1 Controls Both the Secretory Function of the Mammary Gland and Its Remodeling for Successive Gestations [J]. Developmental cell, 2016, 38(5): 522-35.https://doi.org/10.1016/j.devcel.2016.08.005

[28] WESTMAN J, GRINSTEIN S, MARQUES P E. Phagocytosis of Necrotic Debris at Sites of Injury and Inflammation [J]. Frontiers in immunology, 2019, 10(3030.https://doi.org/10.3389/fimmu.2019.03030

[29] GERLACH B D, MARINELLO M, HEINZ J, et al. Resolvin D1 promotes the targeting and clearance of necroptotic cells [J]. Cell death and differentiation, 2020, 27(2): 525-39.https://doi.org/10.1038/s41418-019-0370-1

[30] ABRAHAMS V M, KIM Y M, STRASZEWSKI S L, et al. Macrophages and apoptotic cell clearance during pregnancy [J]. American journal of reproductive immunology (New York, NY : 1989), 2004, 51(4): 275-82.https://doi.org/10.1111/j.1600-0897.2004.00156.x

[31] CHAMLEY L W, CHEN Q, DING J, et al. Trophoblast deportation: just a waste disposal system or antigen sharing? [J]. Journal of reproductive immunology, 2011, 88(2): 99-105.https://doi.org/10.1016/j.jri.2011.01.002

[32] SUN F, WANG S, DU M. Functional regulation of decidual macrophages during pregnancy [J]. Journal of reproductive immunology, 2021, 143(103264.https://doi.org/10.1016/j.jri.2020.103264

[33] VAN DEN BOSSCHE J, O'NEILL L A, MENON D. Macrophage Immunometabolism: Where Are We (Going)? [J]. Trends in immunology, 2017, 38(6): 395-406.https://doi.org/10.1016/j.it.2017.03.001

[34] BATISTA-GONZALEZ A, VIDAL R, CRIOLLO A, et al. New Insights on the Role of Lipid Metabolism in the Metabolic Reprogramming of Macrophages [J]. Frontiers in immunology, 2019,

10(2993.https://doi.org/10.3389/fimmu.2019.02993

[35] MENG Q, GUO P, JIANG Z, et al. Dexmedetomidine inhibits LPS-induced proinflammatory responses via suppressing HIF1α-dependent glycolysis in macrophages [J]. Aging, 2020, 12(10): 9534-48.https://doi.org/10.18632/aging.103226

[36] KORBECKI J, BAJDAK-RUSINEK K. The effect of palmitic acid on inflammatory response in macrophages: an overview of molecular mechanisms [J]. Inflammation research : official journal of the European Histamine Research Society [et al], 2019, 68(11): 915-32.https://doi.org/10.1007/s00011-019-01273-5

[37] REICHHARDT M P, LUNDIN K, LOKKI A I, et al. Complement in Human Pre-implantation Embryos: Attack and Defense [J]. Frontiers in immunology, 2019, 10(2234.https://doi.org/10.3389/fimmu.2019.02234

[38] REGAL J F, BURWICK R M, FLEMING S D. The Complement System and Preeclampsia [J]. Current hypertension reports, 2017, 19(11): 87.https://doi.org/10.1007/s11906-017-0784-4

[39] MAO D, WU X, DEPPONG C, et al. Negligible role of antibodies and C5 in pregnancy loss associated exclusively with C3-dependent mechanisms through complement alternative pathway [J]. Immunity, 2003, 19(6): 813-22.https://doi.org/10.1016/s1074-7613(03)00321-2

[40] USAMI M, MITSUNAGA K, MIYAJIMA A, et al. Complement component C3 functions as an embryotrophic factor in early postimplantation rat embryos [J]. The International journal of developmental biology, 2010, 54(8-9): 1277-85.https://doi.org/10.1387/ijdb.092993mu

[41] MOHLIN F C, GROS P, MERCIER E, et al. Analysis of C3 Gene Variants in Patients With Idiopathic Recurrent Spontaneous Pregnancy Loss [J]. Frontiers in immunology, 2018, 9(1813.https://doi.org/10.3389/fimmu.2018.01813

[42] DONG N, GU H, LIU D, et al. Complement factors and alpha-fetoprotein as biomarkers for noninvasive prenatal diagnosis of neural tube defects [J]. Annals of the New York Academy of Sciences, 2020, 1478(1): 75-91.https://doi.org/10.1111/nyas.14443

[43] BURWICK R M. Complement receptors in pre-eclampsia: cleaning up placental debris [J]. BJOG : an international journal of obstetrics and gynaecology, 2021, 10.1111/1471-0528.16664

[44] PENG S, SUN M, SUN X, et al. Plasma levels of TAM receptors and ligands in severe preeclampsia [J]. Pregnancy hypertension, 2018, 13(116-20.https://doi.org/10.1016/j.preghy.2018.05.012

[45] RETALLACK H, DI LULLO E, ARIAS C, et al. Zika virus cell tropism in the developing human brain and inhibition by azithromycin [J]. Proceedings of the National Academy of Sciences of the United States of America, 2016, 113(50): 14408-13.https://doi.org/10.1073/pnas.1618029113

[46] HASTINGS A K, YOCKEY L J, JAGGER B W, et al. TAM Receptors Are Not Required for Zika Virus Infection in Mice [J]. Cell reports, 2017, 19(3): 558-68.https://doi.org/10.1016/j.celrep.2017.03.058

[47] WELLS M F, SALICK M R, WISKOW O, et al. Genetic Ablation of AXL Does Not Protect Human Neural Progenitor Cells and Cerebral Organoids from Zika Virus Infection [J]. Cell stem cell, 2016, 19(6): 703-8.https://doi.org/10.1016/j.stem.2016.11.011

[48] RYAN N, ANDERSON K, VOLPEDO G, et al. The IL-33/ST2 Axis in Immune Responses Against Parasitic Disease: Potential Therapeutic Applications [J]. Frontiers in cellular and infection microbiology, 2020, 10(153.https://doi.org/10.3389/fcimb.2020.00153

[49] LI Z, ZHOU G, JIANG L, et al. Effect of STOX1 on recurrent spontaneous abortion by regulating trophoblast cell proliferation and migration via the PI3K/AKT signaling pathway [J]. Journal of cellular biochemistry, 2018, 120(5): 8291-9.https://doi.org/10.1002/jcb.28112

[50] DING J, YANG C, ZHANG Y, et al. M2 macrophage-derived G-CSF promotes trophoblasts EMT, invasion and migration via activating PI3K/Akt/Erk1/2 pathway to mediate normal pregnancy [J]. Journal of cellular and molecular medicine, 2021, 25(4): 2136-47.https://doi.org/10.1111/jcmm.16191

[51] HUANG J, XUE M, ZHANG J, et al. Protective role of GPR120 in the maintenance of pregnancy by promoting decidualization via regulation of glucose metabolism [J]. EBioMedicine, 2019, 39(540-51.https://doi.org/10.1016/j.ebiom.2018.12.019

[52] HOMSAK E, GRUSON D. Soluble ST2: A complex and diverse role in several diseases [J]. Clinica chimica acta; international journal of clinical chemistry, 2020, 507(75-87.https://doi.org/10.1016/j.cca.2020.04.011

[53] GRANNE I, SOUTHCOMBE J H, SNIDER J V, et al. ST2 and IL-33 in pregnancy and pre-eclampsia [J]. PloS one, 2011, 6(9): e24463.https://doi.org/10.1371/journal.pone.0024463

[54] ZHU C, WEI Y, WEI X. AXL receptor tyrosine kinase as a promising anti-cancer approach: functions, molecular mechanisms and clinical applications [J]. Molecular cancer, 2019, 18(1): 153.https://doi.org/10.1186/s12943-019-1090-3

Figures

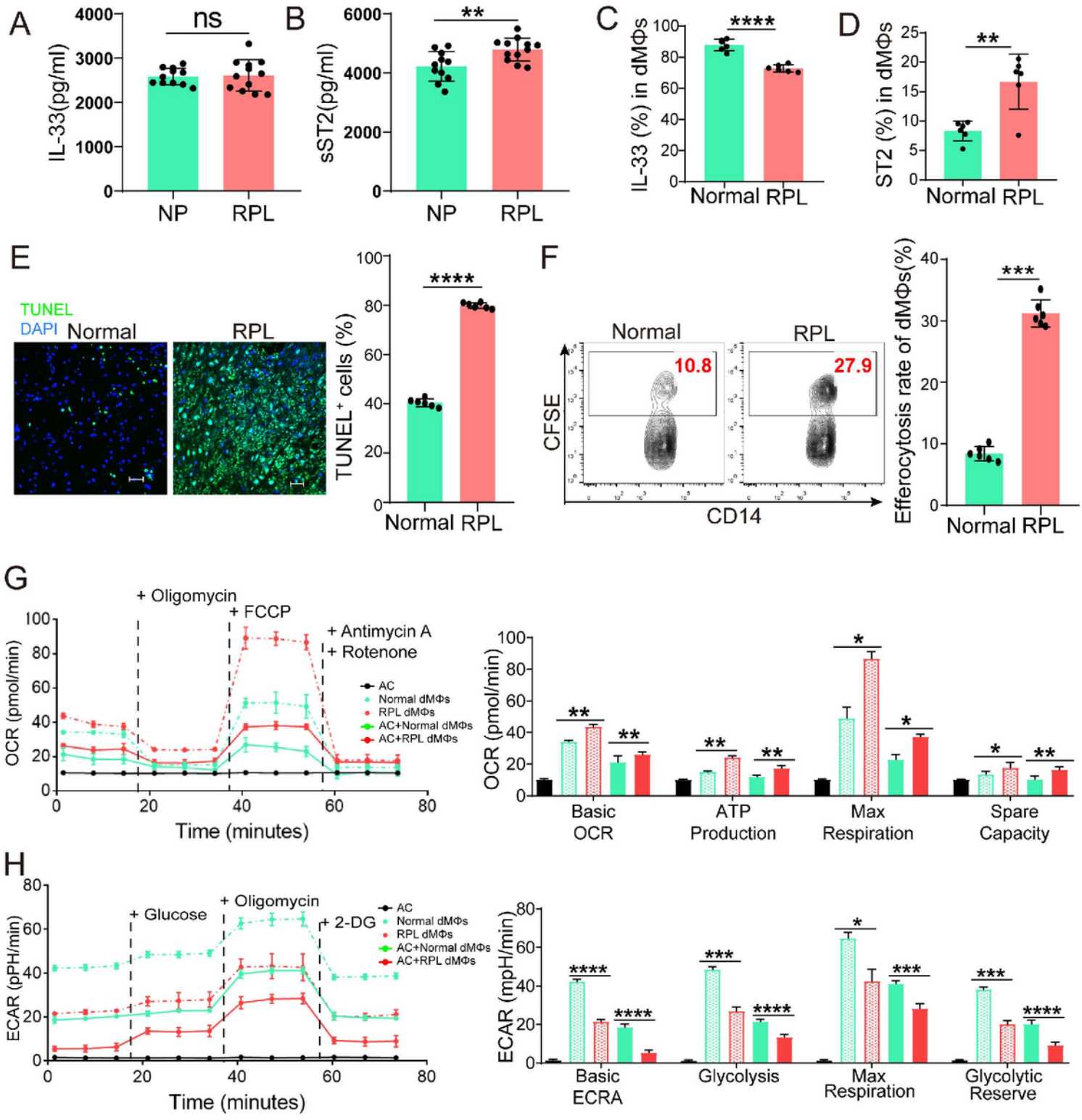

Figure 1

sST2 is increased in the serum of unexplained RPL patients，accompanied with increased apoptotic cells，enhanced efferocytosis and a mitochondrial bias during efferocytosis. Serum from 10 normal pregnancy women and 12 unexplained RPL patients were collected to determine the levels of IL-33 (A) and sST2 (B) by ELISA.The expression of IL-33 (C) and ST2 (D) in dMΦs from normal and unexplained RPL patients were detected by flow cytometry. (E) The number of apoptotic cells at the maternal-fetal interface of

normal and RPL patients tested by TUNEL staining. (F) The efferocytosis ability of dMΦs from normal and RPL patients. (G) The oxidative phosphorylation (OXPHOS) level of efferocytosis metabolism when normal (green solid line) and RPL (red solid line) dMΦs were cocultured with AC or not（indicated by the green dashed and red dashed line respectively). (H) The glycolysis level of efferocytosis metabolism when normal (green solid line) and RPL (red solid line) dMΦs were cocultured with AC or not（indicated by the green dashed and red dashed line respectively). All experiments were performed in triplicate. The data were exhibited as mean ± SD. *P < 0.05, ** P < 0.01, ***P < 0.001, **** P < 0.0001.

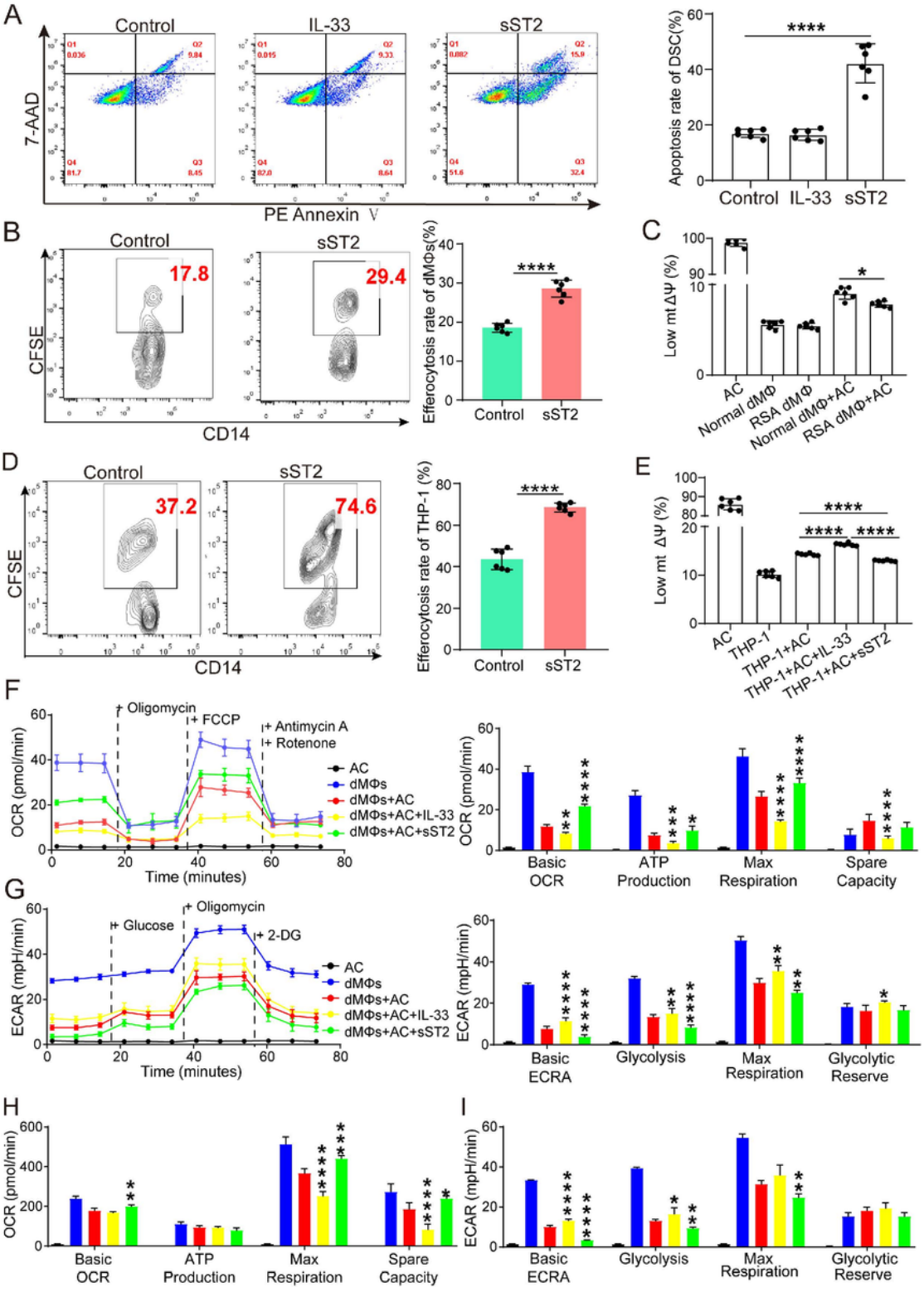

Figure 2

Dysfunction of IL-33/ST2 axis promoted DSCs apoptosis, dMΦs/THP-1 efferocytosis and led to an OXPHOS bias during efferocytosis. (A) The impact of IL-33 (2ng/ml, 48h) and sST2 (200ng/ml,48h) on the apoptosis rate of normal DSCs. (B) The impact of sST2 (200ng/ml,48h) on the efferocytosis of normal dMΦs. (C) The mitochondrial membrane potential (mtΔΨ) of the normal and RPL dMΦs conducting efferocytosis. (D) The impact of sST2 (200ng/ml,48h) on the efferocytosis of THP-1. (E) The impact of IL-33 (2ng/ml, 48h), sST2 (200ng/ml,48h) on the mtΔΨ of THP-1 processing efferocytosis. (F) The OXPHOS level of efferocytosis metabolism affected by IL-33 (2ng/ml, 48h) and sST2 (200ng/ml,48h). (G) The glycolysis level of efferocytosis metabolism affected by IL-33 (2ng/ml, 48h) and sST2 (200ng/ml,48h). The effect of IL-33 (2ng/ml, 48h), sST2 (200ng/ml,48h) on the OXPHOS level (H) and glycolysis level (I) of THP-1 cell line processing efferocytosis. All experiments were performed in triplicate. The data were exhibited as mean ± SD. *P < 0.05, ** P < 0.01, ***P < 0.001, **** P < 0.0001.

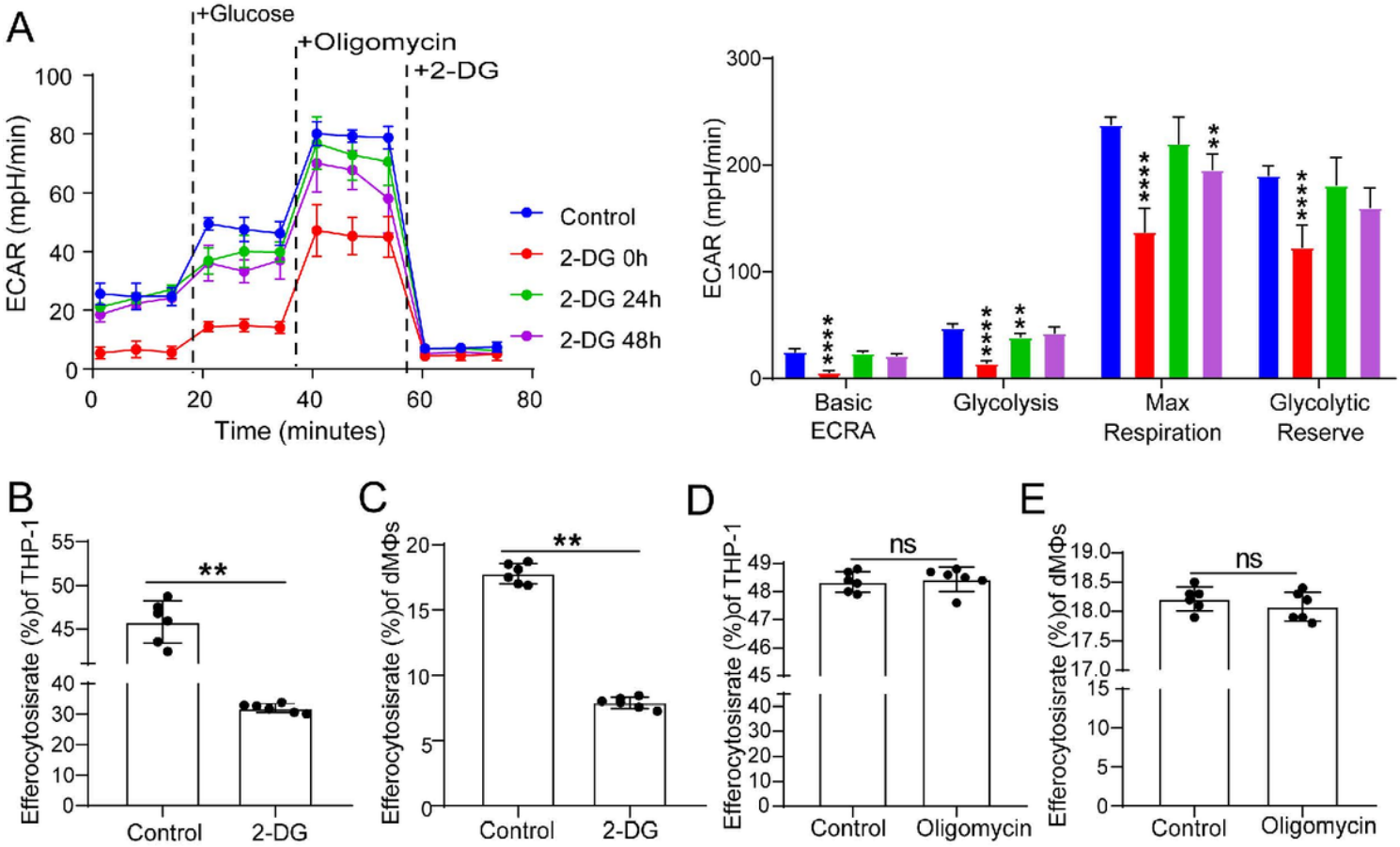

Figure 3

Efferocytosis is more dependent on glycolysis than oxidative phosphorylation. (A) The inhibition efficiency of different treatment duration of 2-DG (10uM) on glycolysis metabolism of THP-1, compared with control group. The impact of 2-DG (10uM) on the efferocytosis of THP-1 (B) and dMΦs (C). The impact of oligomycin (1uM) on the efferocytosis of THP-1 (D) and dMΦs (E). All experiments were performed at least three times. The data were represented as mean ± SD. *P < 0.05, ** P < 0.01, ***P < 0.001, **** P < 0.0001, ns: no statistically significant difference.

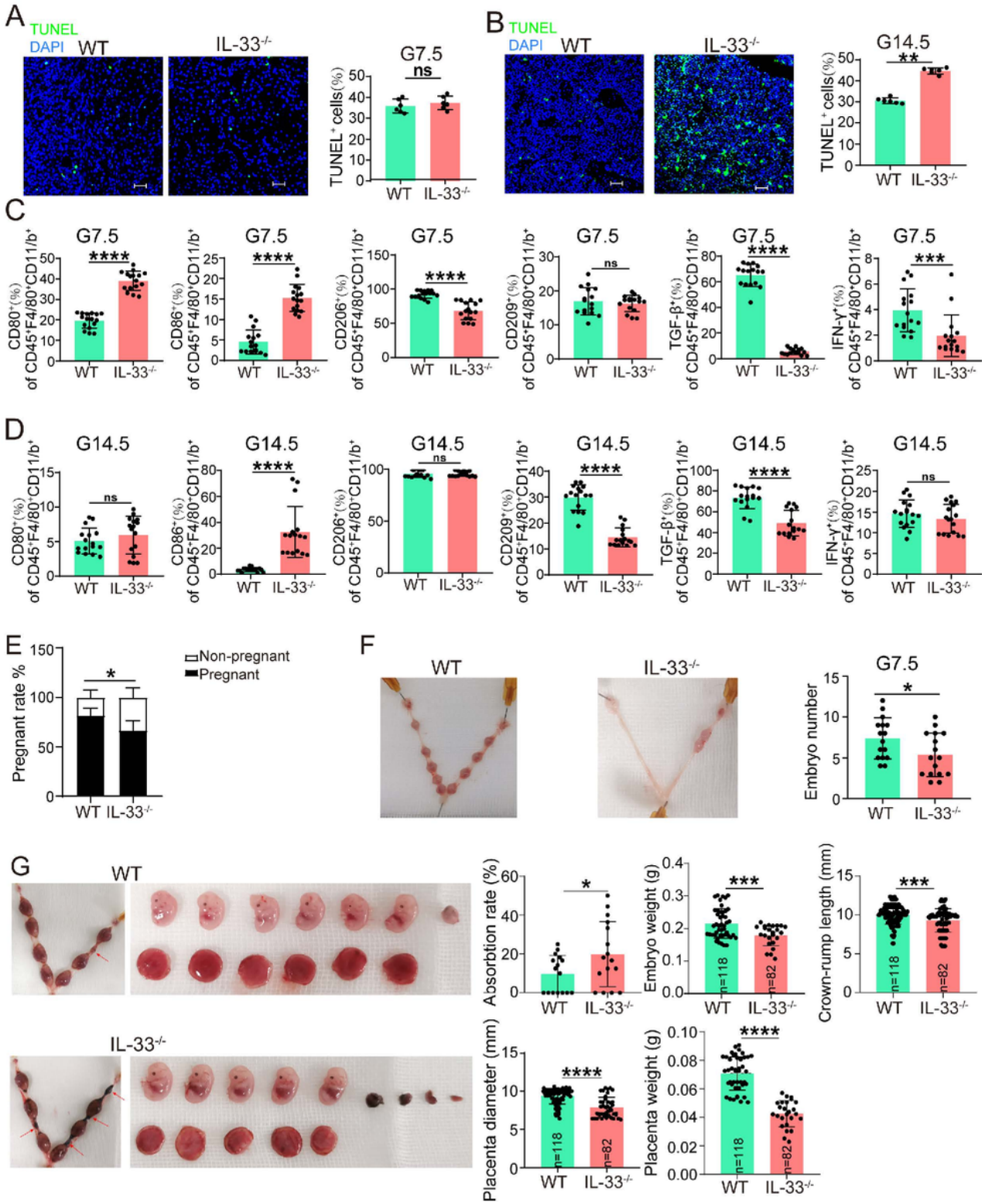

Figure 4

IL-33 deficiency increases the risk of pregnancy failure. The number of apoptotic cells at the maternal-fetal interface of WT and IL-33-/- pregnant mice at G7.5 days (A) and G14.5 days (B) tested by TUNEL staining. The expression of CD80, CD86, CD206, CD209, TGF-β and IFN-γ of CD45+F4/80+CD11/b+ uMΦs from WT and IL-33-/- pregnant mice of G7.5 days (C) and G14.5 days (D). (E) The pregnancy rate of WT and IL-33-/- pregnant mice of G7.5 and G14.5 days. (F) The implantation number of WT and IL-

33-/- pregnant mice of G7.5 days. (G) The embryo absorption rate, weight and crown-rump length of embryos, diameter and weight of placentas of WT and IL-33-/- pregnant mice of G14.5 days. Each experiment was performed at least three times. The data were demonstrated as mean ± SD. *P < 0.05, ** P < 0.01, ***P < 0.001, **** P < 0.0001, ns: no statistically significant difference.

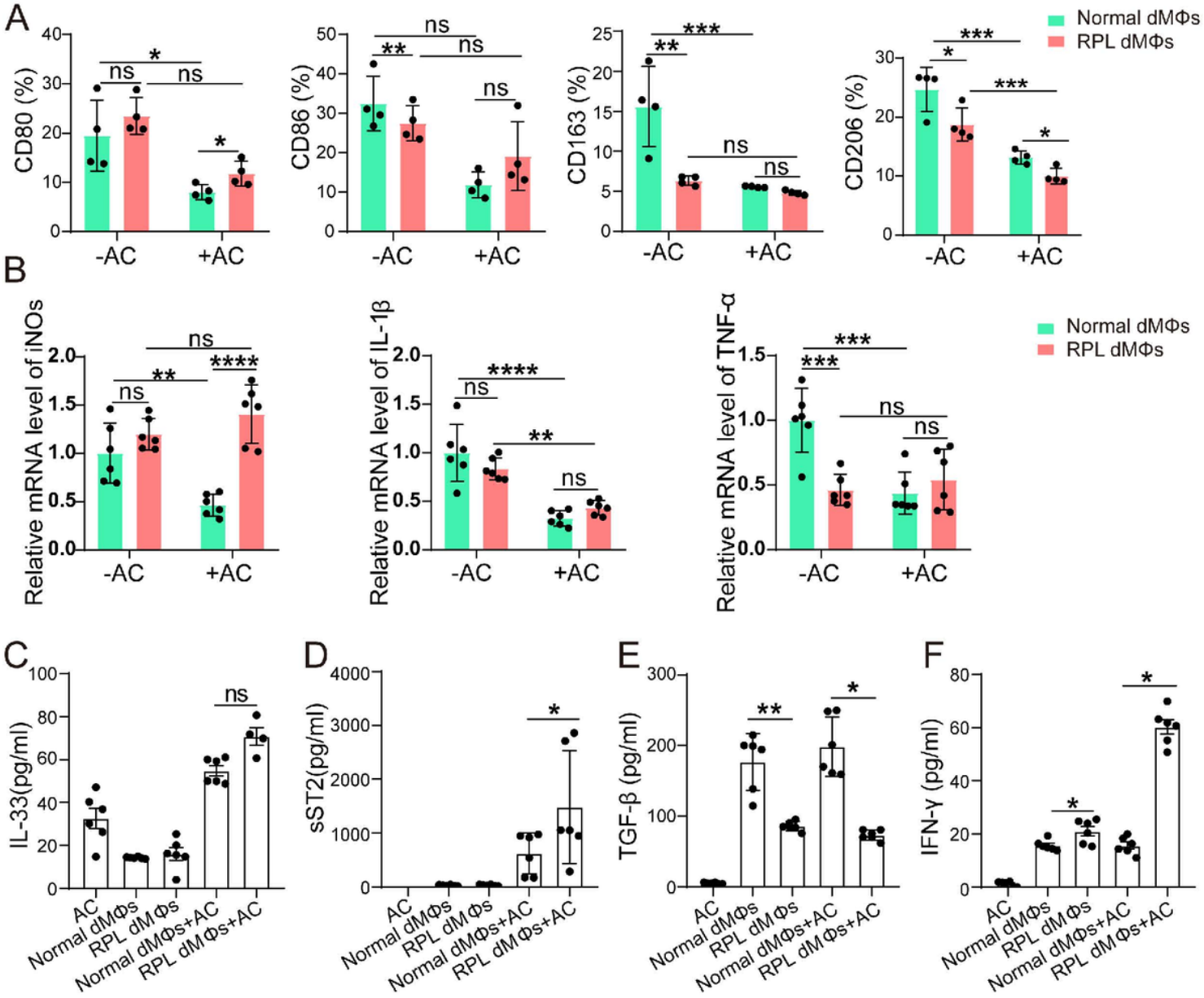

Figure 5

dMΦs from RPL patients is prone to the persistent M1 imbalance and high sST2 after efferocytosis. (A) The expression of CD80, CD86, CD163, CD206 of normal and RPL dMΦs before and after efferocytosis. (B) Quantitative RT-PCR analysis of expression level of iNOS, IL-1β and TNF-α in normal/RPL dMΦs before and after efferocytosis. The concentration of IL-33 (C), sST2 (D), TGF-β(E), IFN-γ (F) in the supernatant of dMΦs before and after efferocytosis. All experiments were conducted at least three times. The data were displayed as mean ± SD. *P < 0.05, ** P < 0.01, ***P < 0.001, **** P < 0.0001, ns: no statistically significant difference.

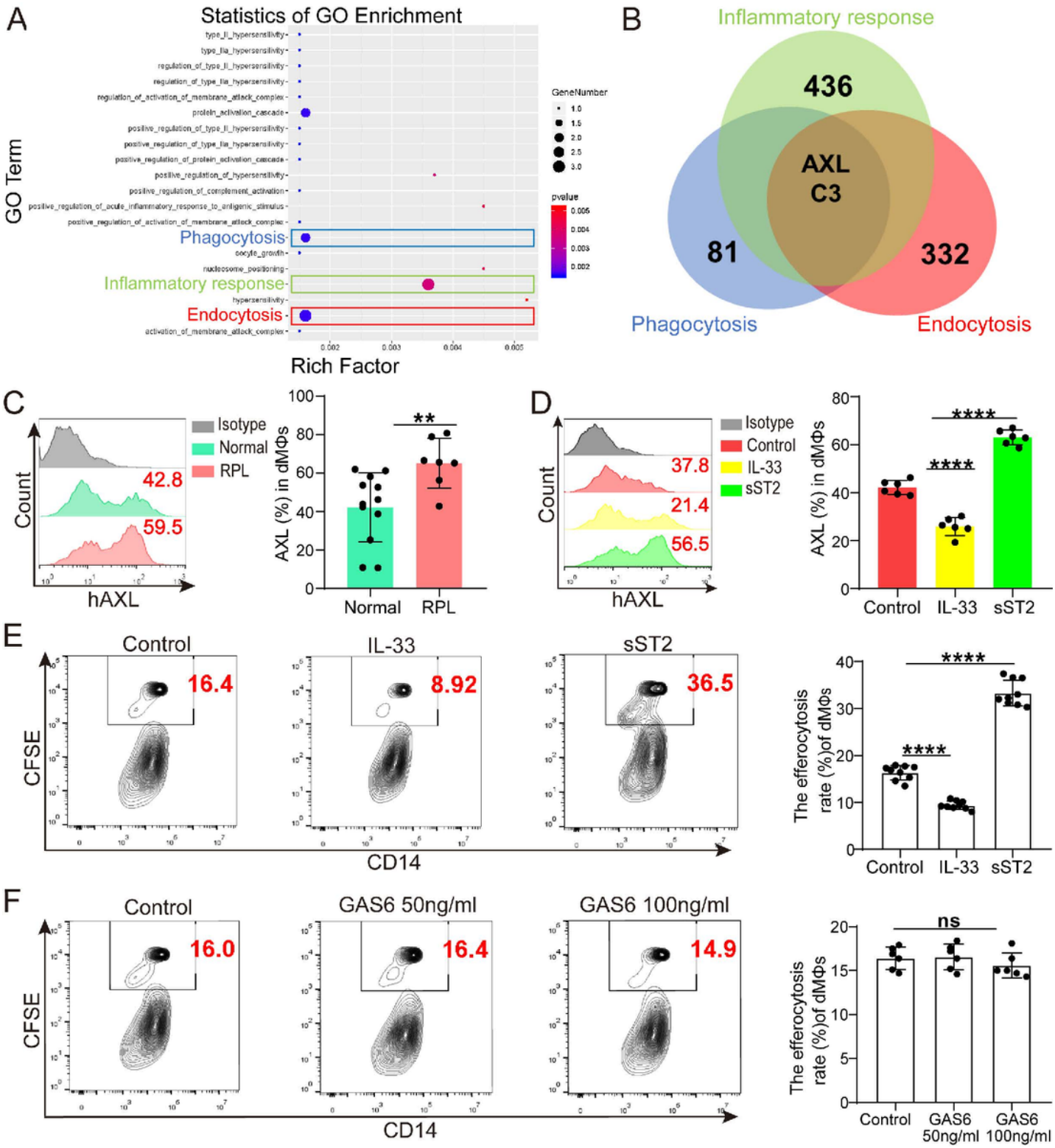

Figure 6

IL-33 suppresses efferocytosis of dMΦs by down-regulating the expression of efferocytosis-related receptor AXL. (A) The GO enrichment analysis diagram of the down-regulated genes. (B) The genes involved in the inflammatory response, phagocytosis and endocytosis pathways were intersected in the form of a Venn diagram. (C)The expression level of human AXL protein of normal and RPL dMΦs. The impact of IL-33 (2ng/ml, 48h) and sST2 (200ng/ml, 48h) on the expression of AXL (D) and the

efferocytosis efficiency (E) of normal dMΦs. (F) The effect of GAS6 (50ng/ml, 100ng/ml, 2h) on the efferocytosis of normal dMΦs. All experiments were performed at least three times. The data were represented as mean ± SD. *P < 0.05, ** P < 0.01, ***P < 0.001, **** P < 0.0001, ns: no statistically significant difference.

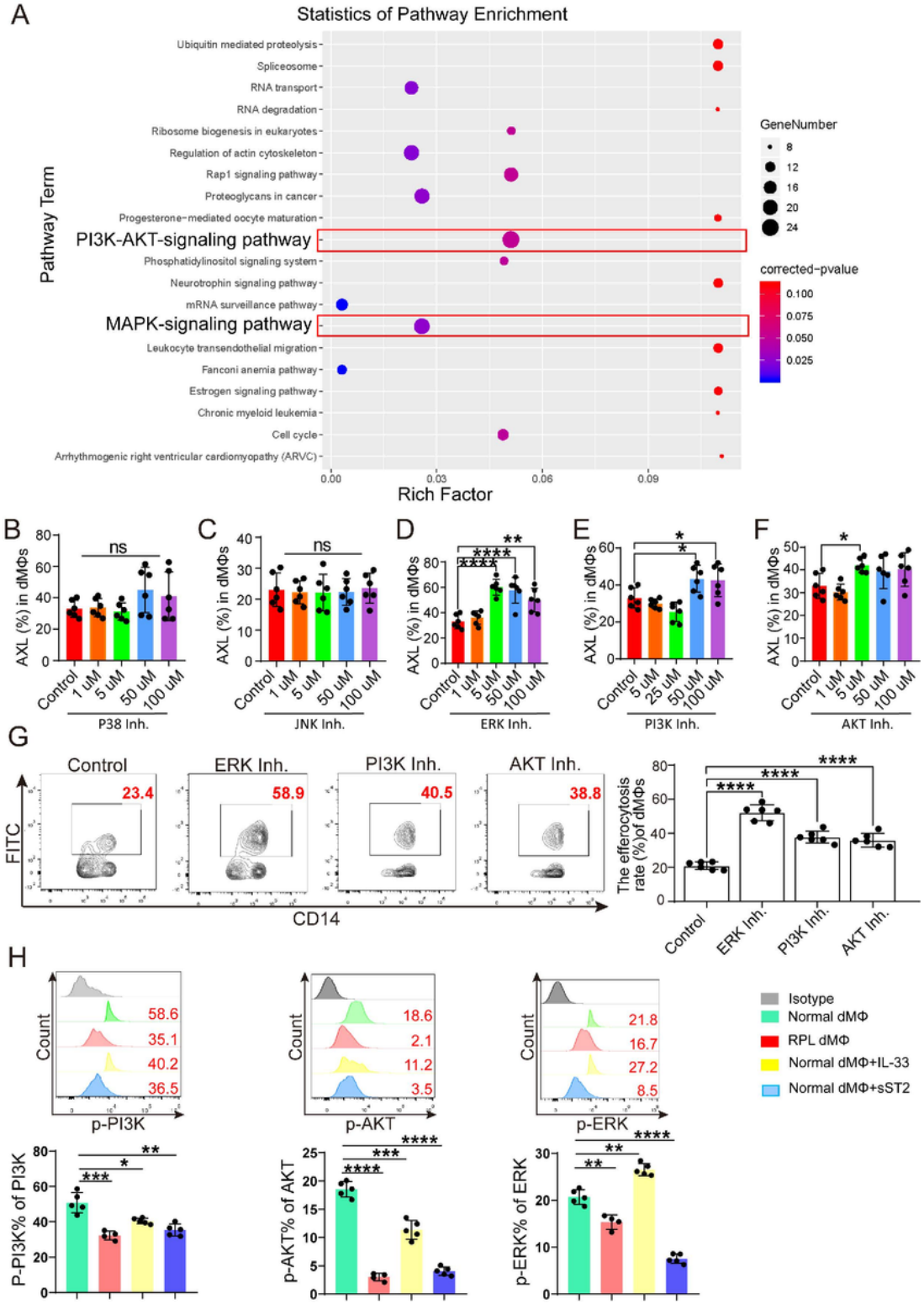

Figure 7

The IL-33/ST2 axis inhibits AXL expression of dMΦs via activating PI3K/AKT and ERK1/2 signaling pathways. (A) The GO enrichment analysis diagram of the up-regulated genes of ST2-OE THP-1 treated with IL-33 for 48h and NC group. The effects of P38 inhibitor (B), JNK inhibitor (C), ERK inhibitor (D), PI3K inhibitor (E), AKT inhibitor (F) at different concentrations on the AXL expression of normal dMΦs. (G) The impact of ERK, PI3K, AKT inhibitor on the efferocytosis efficiency of normal dMΦs. All the inhibitors were cocultured with CD14+ dMΦs for 24h, and during the following 48h, 2ng/ml IL-33 was added in the presence of inhibitors. (H) Normal dMΦs were treated with IL-33 or sST2 for 48h, PI3K, AKT and ERK phosphorylation were analyzed by flow cytometry (n=5), normal and RPL dMΦs without treatment were served as control groups. Each experiment was performed at least three times. The data were represented as mean ± SD after analysis with unpaired t test. *P < 0.05, ** P < 0.01, ***P < 0.001, **** P < 0.0001, ns: no statistically significant difference.

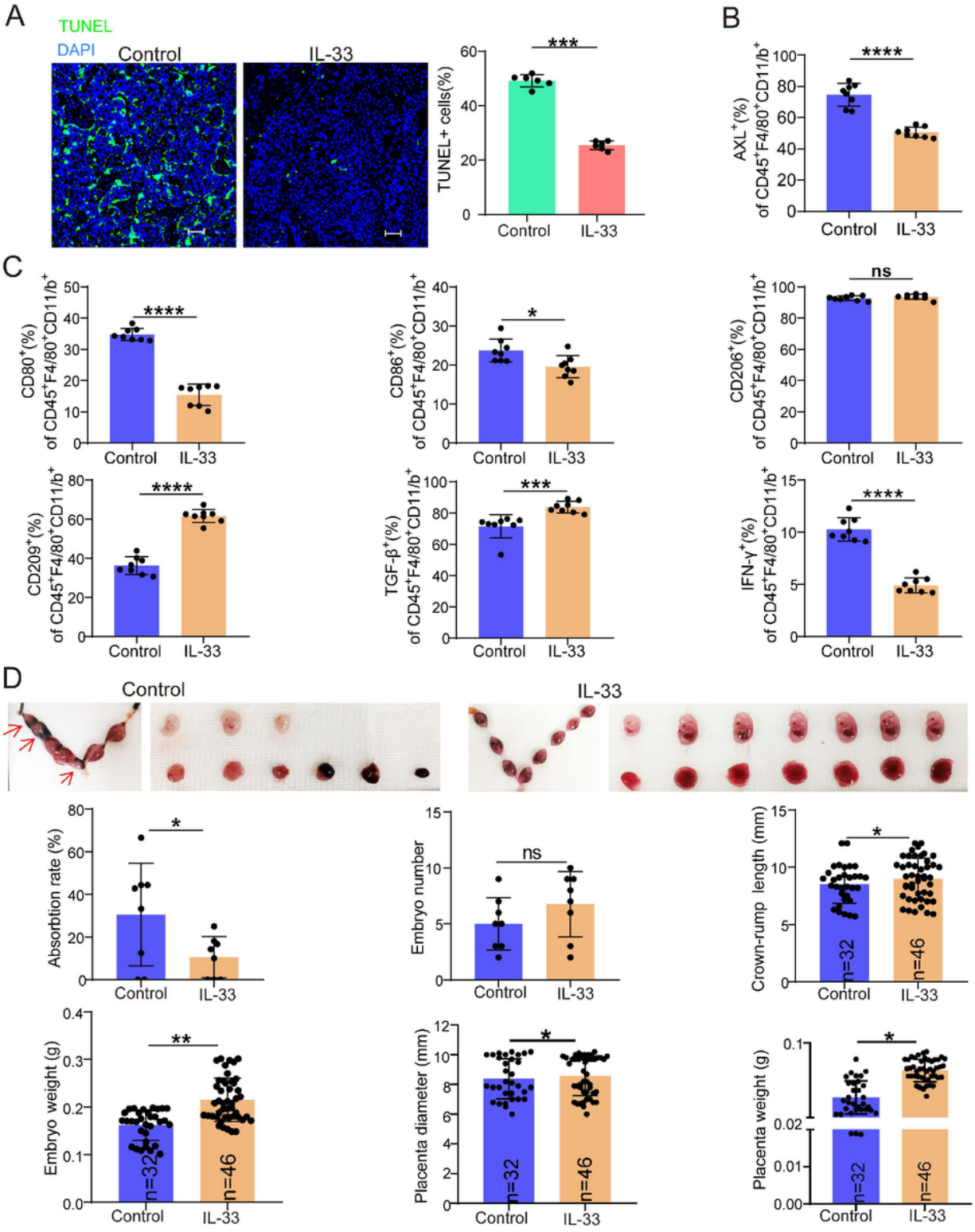

Figure 8

Exogenous IL-33 prevents pregnant failure of IL-33-/- pregnant mice. (A) The number of apoptotic cells at the maternal-fetal interface of IL-33-/- pregnant mice with or without intraperitoneal injection of IL-33 at G14.5 days tested by TUNEL staining. (B) The expression of AXL on CD45+F4/80+CD11/b+ uMΦs from IL-33-/- pregnant mice with or without exogenous peritoneal injection of IL-33 (200ng/100ul, G3.5, G7.5, G11.5) on G14.5 days. (C) The expression of CD80, CD86, CD206, CD209, TGF-β, IFN-γ of

CD45+F4/80+CD11/b+ uMΦs from IL-33-/- pregnant mice with or without exogenous peritoneal injection of IL-33 on G14.5 days. (D) The embryo absorption rate, embryo number, crown-rump length and weight of embryos, diameter and weight of placentas of IL-33-/- pregnant mice with or without exogenous peritoneal injection of IL-33 on G14.5 days. Every experiment was repeated independently at least three times. The data were showed as mean ± SD. *P < 0.05, ** P < 0.01, ***P < 0.001, **** P < 0.0001, ns: no statistically significant difference.

Supplementary Files

This is a list of supplementary files associated with this preprint. Click to download.

- 2021030cleansupplementarymaterials.docx